Circulation Research

ORIGINAL RESEARCH

Overexpression of Wild-Type TMEM43 Improves Cardiac Function in Arrhythmogenic Right Ventricular Cardiomyopathy Type 5

Laura Lalaguna, María Arévalo-Núñez de Arenas, Marina López-Olañeta, María Villalba-Orero, Rafael J. Jiménez-Riobóo, María Victoria Gómez-Gaviro, Joan Isern, Pura Muñoz-Cánoves, Barry J. Byrne, Juan Pablo Ochoa, Pablo García-Pavía, Enrique Lara-Pezzi

BACKGROUND: Arrhythmogenic right ventricular cardiomyopathy type 5 (ARVC5) is the most aggressive type of ARVC, caused by a fully penetrant missense mutation (p.S358L) in TMEM43 (transmembrane protein 43). Pathologically, the disease is characterized by dilation of the cardiac chambers and fibrofatty replacement of the myocardium, which results in heart failure and sudden cardiac death. Current therapeutic options are limited, and no specific therapies targeting the primary cause of the disease have been proposed.

METHODS: We investigated whether overexpression of wild-type (WT) TMEM43 could overcome the detrimental effects of the mutant form. We used transgenic mouse models overexpressing either WT or mutant (S358L) TMEM43 to generate a double transgenic mouse line overexpressing both forms of the protein. In addition, we explored if systemic delivery of a codon-optimized self-complementary adeno-associated virus bearing WT-TMEM43 could improve disease progression assessed by ECG and echocardiography.

RESULTS: Double transgenic mice overexpressing both WT and mutant TMEM43 forms showed delayed ARVC5 onset, improved cardiac contraction, and reduced ECG abnormalities compared with mice expressing S358L-TMEM43. In addition, cardiomyocyte death and myocardial fibrosis were reduced, with an overall increase in survival. Finally, we demonstrated that a single systemic administration of an adeno-associated virus carrying codon-optimized WT-TMEM43 prevents ventricular dysfunction and ECG abnormalities induced by S358L-TMEM43.

CONCLUSIONS: Overexpression of WT-TMEM43 improves the pathological phenotype in a mouse model of ARVC5. Adeno-associated virus-mediated delivery of WT-TMEM43 offers a promising and specific therapy for patients suffering from this highly lethal disease.

GRAPHIC ABSTRACT: A graphic abstract is available for this article.

Key Words: arrhythmogenic right ventricular dysplasia ■ cardiomyopathies ■ mice, transgenic ■ myocardium

Meet the First Author, see p 804 | Editorial, see p 845

Arrhythmogenic right ventricular cardiomyopathy (ARVC) is an inherited cardiac disorder characterized by chamber dilation and fibrofatty replacement of the myocardium. Individuals present with dizziness, ventricular arrhythmias, and sudden cardiac death.[1] A majority of ARVC-associated genetic variants affect proteins of the cardiac desmosome, triggering aberrant signaling pathways that elicit fibrosis and inflammation.[2,3]

Correspondence to: Enrique Lara-Pezzi, PhD, Centro Nacional de Investigaciones Cardiovasculares, Melchor Fernández Almagro, 3, 28029 Madrid, Spain. Email elara@cnic.es

Supplemental Material is available at https://www.ahajournals.org/doi/suppl/10.1161/CIRCRESAHA.124.325848.
For Sources of Funding and Disclosures, see page 843.

Circulation Research is available at www.ahajournals.org/journal/res

Novelty and Significance

What Is Known?

- Arrhythmogenic Right Ventricular Cardiomyopathy type 5 (ARVC5) is a severe cardiac disorder caused by the p.S358L mutation in TMEM43 (transmembrane protein 43).
- Current treatments for ARVC5 are focused on the management of symptoms but fail to address the underlying cause of the disease.

What New Information Does This Article Contribute?

- The p.S358L mutation in TMEM43 does not affect its self-binding ability.
- Overexpression of wild-type TMEM43 significantly improves cardiac function, reduces arrhythmic events, and extends survival in mice.
- This study introduces an effective targeted gene therapy strategy to treat ARVC5 that uses adeno-associated virus (AAVs) to deliver codon-optimized wild-type TMEM43 specifically to cardiomyocytes, offering a potential alternative to palliative treatments.

This study tackles the urgent need for specific therapies in ARVC5 by demonstrating that overexpression of wild-type TMEM43 can counteract the deleterious effects of the p.S358L mutation. Using double transgenic mice and an AAV-based gene delivery system, the authors show marked improvements in cardiac contractility, electrical stability, and survival, alongside reductions in myocardial fibrosis. Importantly, the findings suggest that increasing the proportion of wild-type to mutant TMEM43 within protein complexes may be a key mechanism for rescuing cardiac function. This novel therapeutic approach not only deepens our understanding of ARVC5 pathogenesis but also contributes to the rapidly emerging field of gene therapy strategies to treat inherited cardiac disorders.

Nonstandard Abbreviations and Acronyms

AAV	adeno-associated virus
AAV-LUC	AAV vector expressing luciferase
AAV-MUT	AAV vector expressing S358L-TMEM43
AAV-WT-OPT	codon-optimized wild-type TMEM43 AAV vector
ACTA1	alpha actin 1
ARVC5	arrhythmogenic right ventricular cardiomyopathy type 5
AV	atrioventricular
COL1A1	collagen type I alpha 1 chain
COL3A1	collagen type III alpha 1 chain
GFP	green fluorescent protein
HA	hemagglutinin
LOX	lysyl oxidase
LV	left ventricle
LVEF	left ventricular ejection fraction
POSTN	periostin
TMEM43	transmembrane protein 43
TTR	transthyretin
VP	viral particles
WT	wild-type

Genetic variants of TMEM43 (transmembrane protein 43) are responsible for the most aggressive subtype of the disease, commonly referred to as ARVC type 5 or ARVC5.[4,5] This highly lethal disease has a poor prognosis, especially in men who show a median survival of only 42 years.[6,7] Subjects harboring genetic variants in TMEM43 present an autosomal dominant, fully penetrant form of ARVC, with common left ventricle (LV) involvement.[6–8]

ARVC5 is caused by a point substitution (p.S358L) in a highly conserved transmembrane region of TMEM43.[5] This mutation was initially identified in 2008 in Newfoundland (Canada), but subsequent cases have been diagnosed around the globe, including in Spain, the United Kingdom, Germany, and Denmark.[5,8–10] TMEM43 has 4 transmembrane domains, and the affected serine in ARVC5 (Ser358) lies within the third of these domains. In a previous work, our group reported a transgenic mouse model of ARVC5 that recapitulates the main characteristics of the human disease.[11] Currently, there are no targeted therapies for ARVC5, and only the implantation of an implantable cardioverter-defibrillator (ICD) is offered as a prophylactic treatment to prevent sudden cardiac death. If patients survive ventricular arrhythmia and sudden cardiac death, they often develop end-stage heart failure, and their only alternative is heart transplantation.[2,3]

Here, we investigated the efficacy of wild-type (WT) TMEM43 overexpression as a potential therapy for the treatment of ARVC5. We observed that overexpression of WT-TMEM43 delays the onset of the ARVC5 phenotype in our transgenic mouse model, significantly improving cardiac contraction, reducing ECG abnormalities and fibrosis, and increasing life span. As a first step toward the translation of this finding to the clinics, we generated

an adeno-associated virus (AAV) expressing a codon-optimized WT-TMEM43 that improved the functional and ECG abnormalities caused by S358L-TMEM43. Overall, these data support the therapeutic potential of WT-TMEM43 overexpression in ARVC5 and provide a promising translational tool that could serve as an alternative to current palliative treatments in this highly lethal disease.

METHODS

Please see the Major Resources Table in the Supplemental Material.

Data Availability

The data that support the findings of this study are available from the corresponding author upon reasonable request.

Mice

WT male and female C57BL/6J mice were obtained from the animal facility of Centro Nacional de Investigaciones Cardiovasculares. TMEM43wt and TMEM43mut mice, in the C57BL/6J background, express human WT and human S358L-TMEM43, respectively, specifically in cardiomyocytes under the control of the α-myosin heavy chain promoter, as described previously.[11] Double transgenic mice were obtained by crossing TMEM43wt and TMEM43mut mice. WT littermates were used as controls. Male and female mice were used throughout the study. Genotyping was performed by Sanger sequencing after polymerase chain reaction (PCR) amplification of human *TMEM43* with the following primers: human *TMEM43* forward 5'-TCCCAAGTATCCAGAGGTGGGAGACT-3' and human *TMEM43* reverse 5'-AGGCCGGCAATGAGGAGGG-3' (450 bp amplicon size). Thermocycler conditions were set as follows: initial denaturation at 95 °C for 5 minutes, followed by 37 cycles of denaturation at 98 °C for 30 seconds, annealing at 63 °C for 30 seconds, and extension at 72 °C for 40 seconds.

Mice were housed in an air-conditioned room with a 12-hour light/dark cycle and free access to water and chow. Mice were euthanized in a carbon dioxide chamber. After sacrifice, tibial length was measured, and hearts were weighed. Power calculations were conducted using G*Power software to determine the appropriate sample size required to detect a 10% improvement in ejection fraction, with an SD of ±6.5%, according to previous data.[11] A significance level of 0.05 and 80% power was used for the calculations. Based on these parameters, the required sample size per group was found to be at least 8 animals. Given that ARVC5 often presents differently in women and men, a minimum of 8 animals per sex and group were included in the studies. All procedures were approved by the Ethics Committees of the Centro Nacional de Investigaciones Cardiovasculares and the Regional Government of Madrid (PROEX191.5/22).

Echocardiography

Transthoracic echocardiography was performed in mice aged 5, 10, 16, and 24 weeks. Mice were placed on a heating pad and kept under light anesthesia with isoflurane administered via a nose cone. The anesthesia was adjusted to obtain a target heart rate of 500±50 bpm. Cardiac function, chamber dilation, and wall thickness were analyzed from 2-dimensional and M-mode acquisitions. Image acquisitions were performed by a blinded operator using a high-frequency ultrasound system with a 30-MHz probe (Vevo 2100, Visualsonics). Left ventricular ejection fraction (LVEF) and LV end-diastolic volume measurements were obtained from the long axis view, and LV posterior wall thickness in diastole values were analyzed in the short axis view. Right ventricular systolic function was assessed indirectly from the tricuspid annular plane systolic excursion, estimated from maximum lateral tricuspid annulus movement obtained from a 2-dimensional 4-chamber apical view. Images were analyzed offline by an expert blinded to genotype and treatment using the Vevo 2100 Workstation software.

Electrocardiograms and Flecainide Administration

Mice were anesthetized with isoflurane via nose cone for echocardiography. Surface ECGs were obtained by using bipolar limb leads (leads I, II, and III) and unipolar limb leads (leads aVR, aVL, and aVF) for 90 seconds. Recordings were acquired and analyzed by a blinded operator using Acqknowledge 4.1.1 for MP36R (BIOPAC Systems Inc). Mean values of P-wave duration and amplitude, R-wave and S-wave amplitudes, and QRS duration and amplitude were calculated from 3 nonconsecutive beats from lead II. Mice that exhibited premature ventricular contractions in at least one 90-second ECG recording during follow-up were quantified. For experiments with flecainide, 90-second baseline ECG recordings were obtained before flecainide administration via intraperitoneal injection (40 mg/kg). ECG recordings continued for ≈5 minutes postadministration.

Cell Culture and Immunoprecipitation

TMEM43 co-immunoprecipitation experiments were performed in the P19 cell line. P19 cells were transfected with both HA-tagged and GFP (green fluorescent protein)-tagged TMEM43 WT and S358L constructs using Lipofectamine 2000 (11668019; Thermo Fisher Scientific). Cells were lysed with tris-buffered saline buffer supplemented with 1% IGEPAL, 5 mmol/L EDTA, 5 mmol/L $MgCl_2$, and protease and phosphatase inhibitors (5892791001 and 04906845001, respectively, from Roche) for 30 minutes at room temperature. After centrifugation, the supernatants were precleared with Protein G Dynabeads (10003D; Thermo Fisher Scientific). Proteins were immunoprecipitated with Protein G Dynabeads coupled with a rabbit anti-GFP antibody (632592; Takara Bio), rotating at 4 °C overnight. Beads were washed 3× with 0.05% IGEPAL lysis buffer and 5× with lysis buffer without added detergent. Proteins were eluted from beads by boiling for 5 minutes at 95 °C in Laemmli sample buffer. Input, supernatant, and output samples from the co-immunoprecipitation were resolved by SDS-PAGE.

For TMEM43 codon-optimization experiments, HL1 cells were transfected with plasmids carrying a chicken cardiac troponin T promoter driving GFP, human codon-optimized TMEM43, or human WT TMEM43 expression using jetPRIME transfection reagent (POL101000046; Polyplus).

Western Blots

LV myocardium samples or transfected HL1 cells were homogenized by manual grinding in radioimmunoprecipitation assay buffer in the presence of protease and phosphatase inhibitors (5892791001 and 04906845001, respectively, from Roche). Lysates were separated on 10% SDS-PAGE gels (acrylamide:bisacrylamide 29:1), transferred to polyvinylidene fluoride membranes, and blocked with 3% nonfat dry milk in 1X tris-buffered saline for 1 hour. Membranes were incubated with primary antibodies overnight, followed by appropriate horseradish peroxidase-labeled secondary antibodies (anti-mouse P044701 and anti-rabbit P044801-2; Dako). Horseradish peroxidase activity was detected using Radiance ECL chemiluminescent horseradish peroxidase substrate (AC2204; Azure Biosystems). Primary antibodies were as follows: TMEM43 (ab184164; Abcam), GFP (11814460001; Roche), HA (11583816001; Roche), and vinculin (V4505; Sigma). Blot images were obtained and quantified with the Invitrogen iBright CL750 Imaging System and analysis software (Thermo Fisher Scientific).

RNA Isolation and Quantitative Real-Time PCR

LV samples were snap-frozen in liquid nitrogen right after sacrifice. Total RNA was isolated using TRIzol reagent (15596026; Thermo Fisher Scientific). First-strand cDNA was synthesized using 100 ng of total RNA and a High Capacity cDNA Reverse Transcription Kit (4368814; Thermo Fisher Scientific). Quantitative reverse-transcribed PCR was performed in a QuantStudio 5 real-time PCR thermocycler (Thermo Fisher Scientific) using SYBR Green (4367659; Thermo Fisher Scientific) for double-stranded DNA detection. Primer pairs used for quantitative reverse-transcribed PCR are *LOX* (lysyl oxidase) forward 5'-GCTGCGGAAGAAAACTGC-3' and *LOX* reverse 5'-CCTTGGTTCTTCACTCTTTGC-3' (104 bp amplicon), *POSTN* (periostin) forward 5'-AACGTCTGTGCCCTCCAG-3' and *POSTN* reverse 5'-AGCCTTTCATCCCTTCCATT-3' (151 bp amplicon), *COL1A1* (collagen type I alpha 1 chain) forward 5'-GTGCCACTCTGACTGGAAGA-3' and *COL1A1* reverse 5'-CTGACCTGTCTCCATGTTGC-3' (100 bp amplicon), *COL3A1* (collagen type III alpha 1 chain) forward 5'-CACCCTTCTTCATCCCACTC-3' and *COL3A1* reverse 5'-ATGTCATCGCAAAGGACAGA-3' (159 bp amplicon), *ACTA1* (alpha actin 1) forward 5'-GACCACAGCTGAACGTGAGA-3', *ACTA1* reverse 5'-TGTTGTAGGTGGTCTCATGGAT-3' (239 bp amplicon), and Luciferase forward 5'-TATCATGGCC TCGTGAAATCC-3' and Luciferase reverse 5'-TCCTGGGT CCGATTCAATAAAC-3' (131 bp amplicon). Results were analyzed with the LinReg PCR software,[12] which calculates the PCR efficiency of each sample independently. The average efficiency of each mRNA was then used to calculate the relative expression of each gene, which was normalized to that of β-actin.

Histological Analysis, Immunohistochemistry, and Immunofluorescence

Hearts were fixed in 4% paraformaldehyde in PBS for 48 hours, washed in PBS, dehydrated, included in paraffin, and sliced in 5 µm sections. The collagen content was analyzed using Masson trichrome protocol.[13] For immunofluorescence, heart sections were subjected to sodium citrate antigen retrieval, permeabilized with 0.1% Tween-20/PBS for 20 minutes, and blocked with blocking solution (5% goat serum, 2% $MgCl_2$, 3% BSA in 0.3% Tween-20/PBS). Sections were incubated with anti-TMEM43 (ab184164; Abcam) diluted 1:100, followed by secondary antibody Alexa 568-labeled goat anti-rabbit (A-11011; Thermo Fisher Scientific) diluted 1:200, and wheat germ agglutinin (WGA) Alexa Fluor 488 conjugate (W11261, Thermo Fisher Scientific) diluted 1:2000. Nuclei were stained with DAPI (4′,6-diamidino-2-phenylindole; D1306; Thermo Fisher Scientific). Samples were mounted in Vectashield mounting medium (H-1000; Vector Laboratories). Antibody-negative tissue sections were used as a control for the primary antibody, while a secondary-only control was included to account for nonspecific binding of the secondary antibody.

Immunofluorescence images were acquired with a Leica SP5 confocal microscope, an HCX PL APO CS 10× 0.4 dry objective, and Leica LAS-AF 2.7.3 software. Images for immunohistochemistry were digitized with NanoZoomer-2.0RS (Hamamatsu). All images were analyzed offline with Fiji, and brightness and contrast were linearly adjusted.

Brillouin Spectroscopy

Brillouin spectra were acquired with a home-modified Olympus BX51 reflected light microscope with a diode-pumped solid-state (DPSS) laser at 532 nm (SpectraPhysics) and a light power below 3.5 mW on the sample coupled to a 3+3 TandemFabry-Perot spectrometer (J. Sandercock, Table Stable Ltd.).[14,15] An Olympus MPlan 10X objective with a numerical aperture of 0.25 was used to focus the incident light beam and to collect the scattered light simultaneously. Measurements were performed on dried samples to avoid having to account for water content variability. The tip of the heart apex was carefully sliced to allow the entry of agarose into the ventricular lumen, and samples were embedded in agarose (0.2 g/10 mL distilled water) and sliced into 500 µm sections using a vibratome (Campdem Instruments). A cover slip was placed on top of the sample without sealing. Transparent nail polish was applied on the sides to fix the cover slip. Samples were dried out at room temperature for 5 hours and stored at 4 °C overnight. Brillouin frequency shift, its error, and the half width half maximum were obtained from the Brillouin spectra by a nonlinear least squares fitting procedure using a Pseudo-Voigt function and a cubic polynomial background in MATLAB environment. Laboratory temperature monitoring, displacement of the Märzhäuser Wetzler automated table, and the GHOST multichannel analyzer were controlled with our own developed software using LABVIEW 4 platform.

AAV Vector Production and Delivery

Codon optimization of human *TMEM43* was performed using VectorBuilder design studio. Self-complementary AAV vectors codon-optimized wild-type *TMEM43* AAV vector (AAV-WT-OPT), AAV vector expressing S358L-TMEM43 (AAV-MUT), and AAV vector expressing luciferase (AAV-LUC) expressing optimized human WT-TMEM43, S358L-TMEM43, and luciferase, respectively, were constructed by VectorBuilder. Centro Nacional de Investigaciones Cardiovasculares's Viral Vector Unit produced the recombinant AAVs with the AAVMYO myotropic capsid[16] in-house using a modified Rep/Cap vector.

Briefly, the cap gene from the AAV9 variant in the pAAV2/9n helper plasmid (gift from James M. Wilson, addgene number 112865) was replaced by digestion and ligation with a 3014-bp SwaI+SbfI fragment encoding the AAVMYO viral particle 1 (VP1) gene (obtained by synthesis from the public GenBank sequence deposited under accession: MN365014).

For viral administration, neonatal mice at postnatal day 1 (P1) were lightly anesthetized with ice, and 30 uL of the viral preparation, including 5e10 VP, were injected through the temporal vein in a single injection (1.7e13 VP/kg). Neonates recovered on a heating mat before placing them back together with the dams.

For experiments involving symptomatic adult mice, a subgroup of AAV-MUT mice was randomized into 2 subgroups based on LVEF and QRS amplitude at 10 weeks of age. Mice without signs of disease at this time were excluded from the study (n=7). These subgroups were then treated with 1.7e13 VP/kg of either AAV-LUC or AAV-WT-OPT via the femoral vein.

Statistical Analysis

All statistical analyses were performed using GraphPad Prism (version 10.0.0; GraphPad Software). Data sets were first assessed for normality using the Shapiro-Wilk test. For data meeting the assumption of normality, statistical significance was evaluated using regular 1-way or 2-way ANOVA, followed by Bonferroni posttest for multiple comparisons. For non-normally distributed data, the Kruskal-Wallis test followed by Dunn multiple comparisons test, or multiple Mann-Whitney *U* tests with Bonferroni-Dunn posttest for multiple comparisons, were used as specified in the figure legends. Survival curves were analyzed using the log-rank (Mantel-Cox) test.

Statistical significance was defined as $P<0.05$, and exact *P* values were provided where applicable. Data are presented as mean±SD.

RESULTS

WT-TMEM43 Overexpression in the Heart Improves Cardiac Contractility, Reduces Electrophysiological Abnormalities, and Extends Life Span

We have previously shown using in silico models that WT-TMEM43 and S358L-TMEM43 can form heterodimers. To confirm the models experimentally, we conducted IP experiments using tagged proteins to increase specificity. We found that GFP-tagged S358L-TMEM43 co-immunoprecipitated with HA-tagged S358L-TMEM43 as well as with HA-tagged WT-TMEM43 (Figure 1A). This result validated the in silico models and led us to hypothesize that the overexpression of WT-TMEM43 might quench the deleterious dominant effects of the mutant protein by forming a heterodimer.

To explore whether WT-TMEM43 overexpression could reduce the toxicity of S358L-TMEM43, we crossed our ARVC5 mouse model overexpressing human S358L-TMEM43 (TMEM43mut) with mice overexpressing human WT-TMEM43 (TMEM43wt mice) to generate a double transgenic mouse line that overexpresses both forms of the human protein in a cardiac-specific manner. The functional effects were evaluated through echocardiography and ECG over 24 weeks, and double transgenic mice were compared with TMEM43mut, TMEM43wt, and WT littermates.

The life span of double transgenic mice increased significantly by >10 weeks compared with mice overexpressing the mutant TMEM43, with a median life span of 34.6 versus 23.9 weeks, respectively (Figure 1B). Echocardiography analysis revealed improved LV contraction (LVEF) and reduced dilation in double transgenic mice (Figure 1C and 1D, respectively), while LV wall thickness remained unaltered in all of the groups (Figure 1E). Right ventricular contractility was also improved in double transgenic mice, without any significant deterioration observed until 24 weeks of age (Figure 1F). In addition, double transgenic mice exhibited reduced heart weight to tibial length ratio compared with TMEM43mut mice (Figure 1G).

Overexpression of WT-TMEM43 also improved ECG abnormalities caused by the mutant protein (Figure 2A through 2D). In contrast to the progressive P-wave prolongation observed in TMEM43mut mice, double transgenic mice exhibited normal P-wave duration (Figure 2B). Similarly, double transgenic mice showed reduced QRS duration and increased QRS amplitude compared with TMEM43mut mice at both 16 and 24 weeks of age (Figure 2C and 2D). Furthermore, the proportion of mice showing premature ventricular contractions, a common pathological manifestation in ARVC5 patients, was reduced to levels found in WT mice among double transgenic mice (≈12.5%), compared with TMEM43mut mice (≈35%) (Figure S1A and S1B). In line with these results, the mislocalization of connexin 43 observed in TMEM43mut mice was also partially prevented in double-transgenic mice (Figure S2).

WT-TMEM43 Overexpression Reduces Myocardial Fibrosis

As we previously demonstrated, ARVC5 mice develop extensive myocardial fibrosis as a result of cardiomyocyte death, evidenced by an increase in circulating cardiac troponin I levels.[11] As shown in Figure 3A, double transgenic mice showed a delayed rise in circulating troponin I compared with mutant mice, in agreement with the delayed onset of the disease. Moreover, double transgenic mice presented reduced expression of fibrosis markers at week 16, including *LOX*, which is responsible for collagen and elastin crosslinking, *POSTN*, and collagens 1 and 3 (*COL1A1* and *COL3A1*), together with a decrease of the cardiac stress marker *ACTA1* (Figure 3B through 3F). Masson trichrome staining confirmed a reduced fibrotic content in the heart of double transgenic mice compared with TMEM43mut mice at both 16 and 24 weeks (Figure 4A through

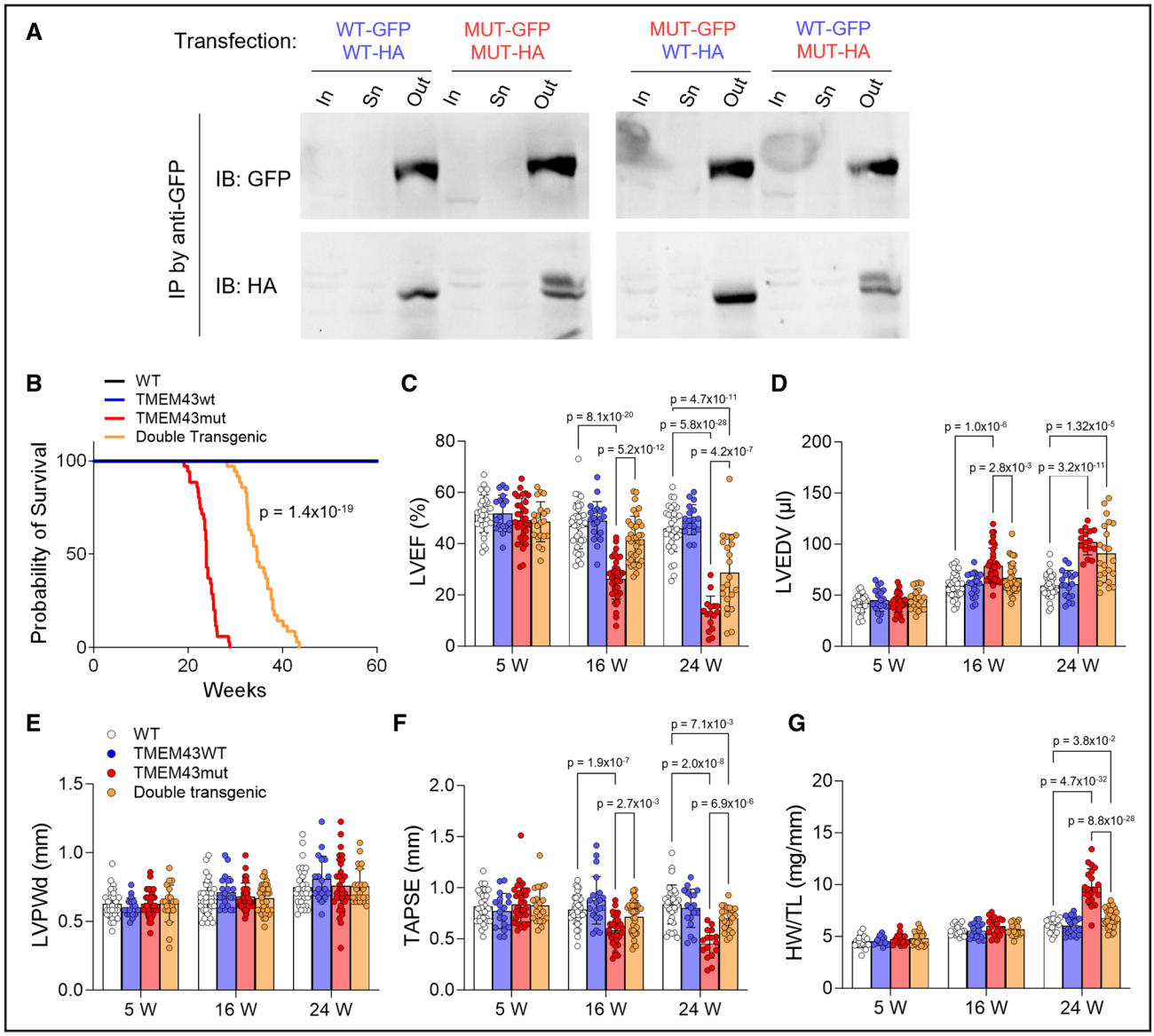

Figure 1. Wild-type (WT) TMEM43 (transmembrane protein 43) overexpression improves systolic function and life span in arrhythmogenic right ventricular cardiomyopathy type 5 (ARVC5) mice.

A, Anti-GFP (green fluorescent protein) co-immunoprecipitation in protein extracts from P19 cells transfected with GFP- and HA-tagged WT (blue) or S358L (MUT, red) TMEM43. Input (In), supernatant (Sn), and output (Out) from the IP (immunoprecipitation) were analyzed by Western blot. TMEM43 was detected by Western blot with antibodies against GFP and HA. **B**, Survival rate of WT mice (n=22), mice overexpressing either WT-TMEM43 (TMEM43wt, n=20) or S358L-TMEM43 (TMEM43mut, n=35), and double-transgenic mice (n=35). The indicated *P* value was obtained with a log-rank test. **C** through **F**, Left ventricular ejection fraction (LVEF, **C**), left ventricle end-diastolic volume (LVEDV, **D**), left ventricle posterior wall thickness in diastole (LVPWd, **E**), and tricuspid annular plane systolic excursion (TAPSE, **F**) measured by echocardiography at 5, 16, and 24 weeks of age. n=16 to 36, each group. **G**, Ratio of heart weight to tibial length (HW/TL) determined at 5, 16, and 24 weeks. n=13 to 31, each group. Data are shown as mean±SD. Two-way ANOVA followed by Bonferroni posttest (**C** and **G**) or multiple Mann-Whitney *U* tests followed by Bonferroni-Dunn posttest (**D**, **E**, and **F**) were used. Since there is no significant difference between WT and TMEM43wt mice, statistical comparisons between TMEM43wt and TMEM43mut or double transgenic mice are omitted to enhance the clarity of the plots. HA indicates hemagglutinin; and IB, immunoblot.

4E). Consistent with these results, TMEM43mut mice showed an increased Brillouin frequency shift, indicating increased stiffness of the myocardial tissue compared with double transgenic, WT, and TMEM43wt mice (Figure 4F). Together, these results demonstrate that WT-TMEM43 overexpression reduces cardiomyocyte death, fibrotic replacement, and myocardial stiffness, leading to improved cardiac function.

WT-TMEM43 Expression Is Enhanced by Codon Optimization

After the positive impact of WT-TMEM43 overexpression in our ARVC5 mice, we developed a gene therapy tool based on AAVs carrying WT-TMEM43 to further explore the therapeutic potential of this approach. To enhance vector efficiency, we first investigated the influence of

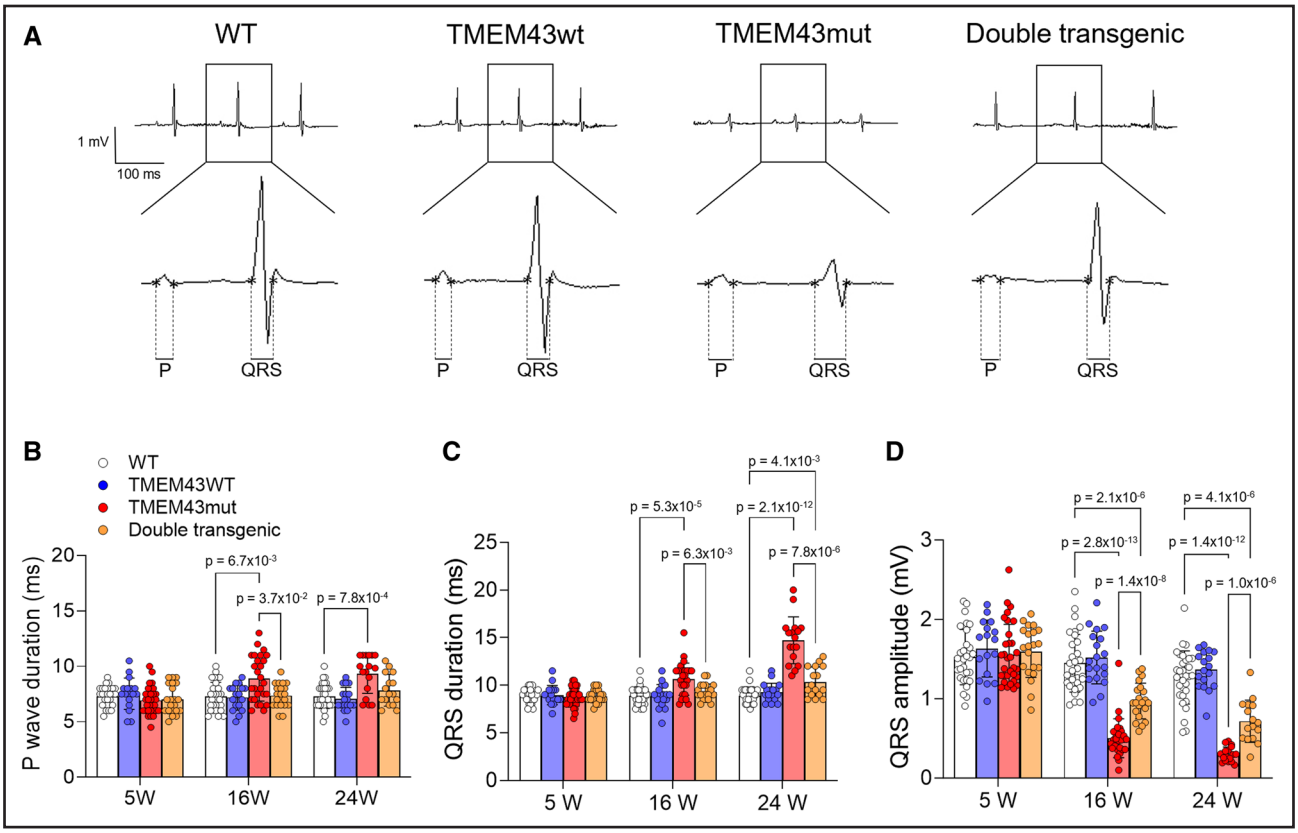

Figure 2. Wild-type (WT) TMEM43 (transmembrane protein 43) overexpression reduces ECG abnormalities in arrhythmogenic right ventricular cardiomyopathy type 5 (ARVC5) mice.

A, Surface ECG traces and magnifications from lead II in 16-week-old mice. **B** through **D**, P-wave duration (**B**) and QRS duration and amplitude (**C** and **D**) were measured from lead II surface electrocardiograms. n=16 to 32, each group. Data are shown as mean±SD. Multiple Mann-Whitney *U* tests were used, followed by Bonferroni-Dunn posttest. Since there is no significant difference between WT and TMEM43wt mice, statistical comparisons between TMEM43wt and TMEM43mut or double transgenic mice are omitted to enhance the clarity of the plots.

cDNA codon optimization on the expression of human WT-TMEM43. This process includes substituting rare or nonpreferred codons in the original cDNA sequence with synonymous codons that are more frequently used by the host, likely improving mRNA stability and protein translation efficiency without altering the encoded protein's amino acid sequence.[17] HL1 cells were transfected with control (GFP), human TMEM43 (TMEM43WT), and codon-optimized human TMEM43 (TMEM43WT-OPT) constructs, and protein expression was assessed through western blot. Our results revealed a positive impact of codon optimization on TMEM43 protein expression (Figure S3A and S3B), prompting the utilization of this optimized sequence for the development of a self-complementary myotropic AAV. This vector expresses codon-optimized TMEM43 specifically in the cardiac tissue under the control of the cardiac troponin T promoter, hereafter referred to as AAV-WT-OPT (Figure S3C).

AAV-WT-OPT Prevents Systolic Dysfunction and ECG Abnormalities Caused by Mutant TMEM43

To determine the efficacy of our gene therapy approach and ensure a similar ratio of WT to mutant human TMEM43, we used systemic delivery of myotropic AAVs in neonates through the temporal vein and followed the animals for 24 weeks (Figure 5A). Each neonate received a total of 5e10 VP distributed as follows: 2.5e10 VP of AAV-WT-OPT+2.5e10 VP of AAV-LUC, 2.5e10 VP of AAV carrying S358L-TMEM43 (AAV-MUT)+2.5e10 VP of AAV-LUC, or 2.5e10 VP of AAV-WT-OPT+2.5e10 VP of AAV-MUT.

Western blot and PCR analyses revealed sustained TMEM43 overexpression in mice infected with AAV-WT-OPT or AAV-MUT (Figure 5B; Figure S4). Similarly, mice infected or co-infected with AAV-LUC expressed high levels of luciferase mRNA, as determined by quantitative reverse-transcribed PCR (Figure 5C). Immunofluorescence analysis of human TMEM43 showed overexpression of the protein in 10% to 30% of cardiomyocytes (Figure 5D through 5K), indicating wide biodistribution of the viral infection and cell type-specific protein expression.

Consistent with our TMEM43mut transgenic mice, mice transduced with AAV-MUT+AAV-LUC showed reduced life span (Figure 6A) and a progressive decline in LVEF as assessed by echocardiography (Figure 6B). This cardiac function impairment and life span decline were successfully prevented in mice co-infected with

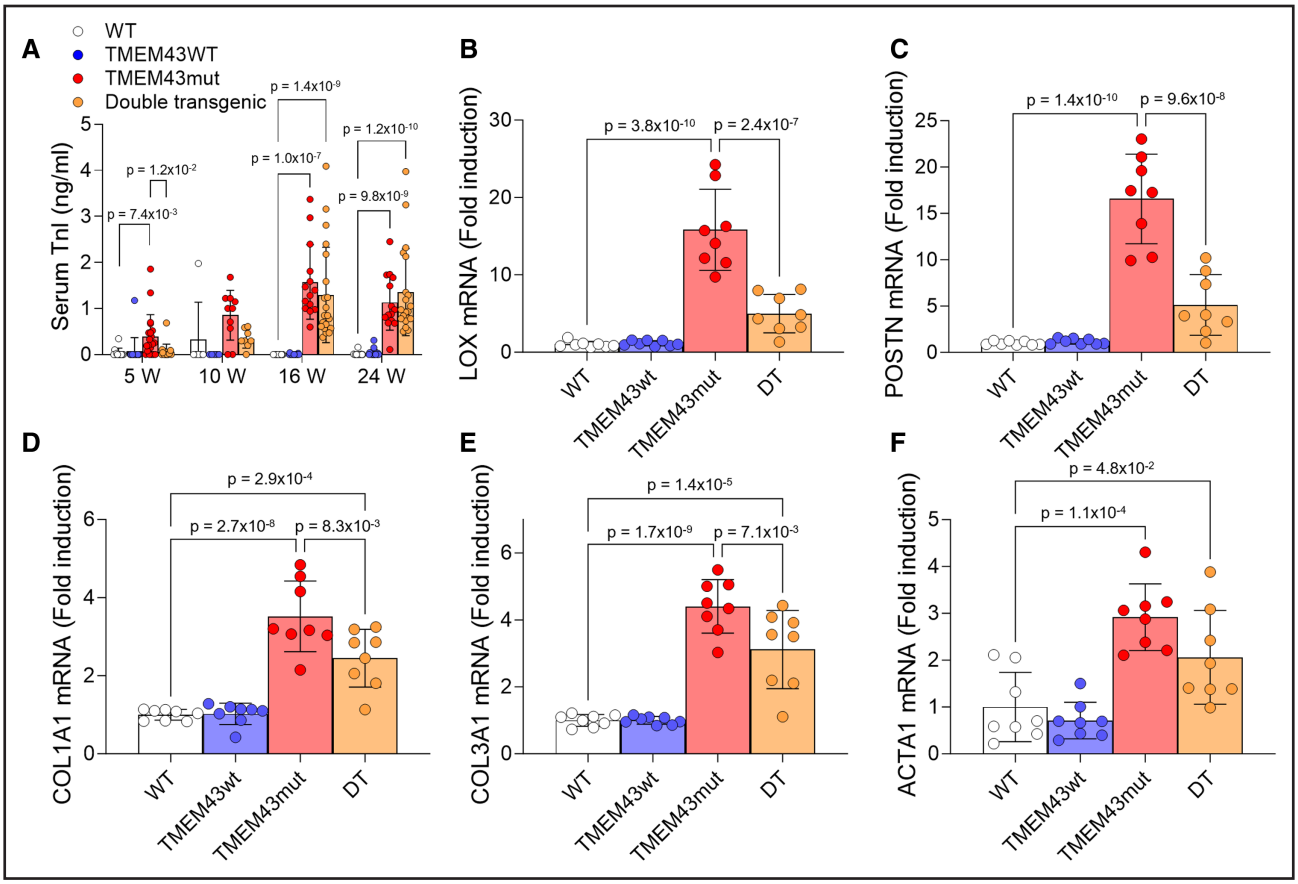

Figure 3. Wild-type (WT) TMEM43 (transmembrane protein 43) overexpression results in reduced cardiomyocyte death and downregulation of fibrosis-related genes.
A, Serum troponin I (TnI) levels were measured by ELISA in mice at 5, 10, 16, and 24 weeks of age. n=6 to 21, each group. **B** through **F**, mRNA expression levels of *LOX* (lysyl oxidase, **B**), *POSTN* (periostin, **C**), *COL1A1* (collagen type I alpha 1 chain, **D**), *COL3A1* (collagen type III alpha 1 chain, **E**), and *ACTA1* (alpha actin 1, **F**) were determined by quantitative reverse-transcribed polymerase chain reaction in 16-week-old mouse hearts. n=8, each group. Data are shown as mean±SD. Multiple Mann-Whitney *U* tests followed by Bonferroni-Dunn posttest (**A**) or 1-way ANOVA followed by Bonferroni posttest (**B** through **F**) were used. Since there is no significant difference between WT and TMEM43wt mice, statistical comparisons between TMEM43wt and TMEM43mut or double transgenic (DT) mice are omitted to enhance the clarity of the plots.

AAV-WT-OPT+AAV-MUT, providing additional support for the therapeutic potential of WT-TMEM43 overexpression. Right ventricular function showed similar trends, although the differences were milder and did not reach statistical significance (Figure 6C). AAV-MUT mice also developed ECG abnormalities, including increased P-wave duration, progressive widening of the QRS, and a gradual decline of the QRS amplitude, mirroring the pathological changes observed in our TMEM43mut transgenic mice. Remarkably, coadministration of AAV-WT-OPT proved sufficient to prevent all these ECG abnormalities (Figure 6D through 6G). In addition, the proportion of mice showing premature ventricular contractions during follow-up was reduced in AAV-WT-OPT+AAV-MUT coinfected mice compared with AAV-MUT mice (Figure S5).

AAV-WT-OPT Prevents Cardiomyocyte Necrosis and Upregulation of Fibrosis-Related Genes

AAV-MUT mice also showed a significant increase in circulating cardiac troponin I levels, albeit to lower levels than TMEM43mut transgenic mice (Figure 7A). This cardiomyocyte death was accompanied by mild but significant increases in the expression of genes related to fibrosis, including *LOX*, *POSTN*, and collagens 1 and 3, and the cardiac stress marker *ACTA1* (Figure 7B through 7F). Importantly, coinfection with AAV-WT-OPT+AAV-MUT strongly reduced cardiomyocyte death and partially prevented the induction of fibrosis and stress genes (Figure 7A through 7F). Collectively, these findings support that AAV-WT-OPT gene therapy can prevent cardiomyocyte necrosis and the upregulation of fibrosis-related genes, improving cardiac contraction and reducing ECG abnormalities, in agreement with the results obtained in the double transgenic mice.

Treatment of Adult Symptomatic ARVC5 Mice With AAV-WT-OPT Improves Systolic Function and Reduces Arrhythmia Susceptibility

To date, we have demonstrated the potential of WT-TMEM43 overexpression as a preventive therapeutic

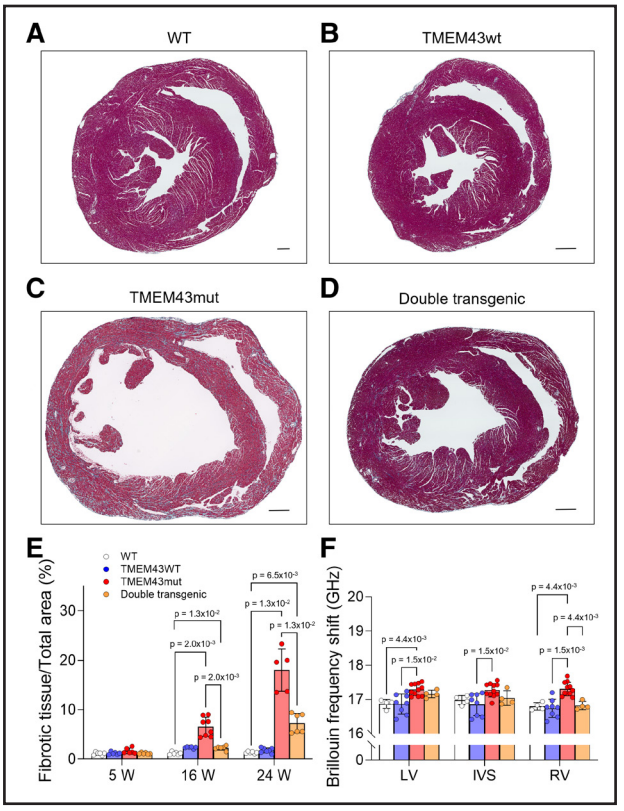

Figure 4. Wild-type (WT) TMEM43 (transmembrane protein 43) overexpression reduces myocardial fibrosis in arrhythmogenic right ventricular cardiomyopathy type 5 (ARVC5) mice.

A through **D**, Collagen content in myocardial cross-sections from WT (**A**), TMEM43wt (**B**), TMEM43mut (**C**), and double transgenic (**D**) mice was analyzed at 24 weeks of age by Masson trichrome staining; scale bar, 500 µm. **E**, Quantification of fibrotic tissue from Masson trichrome staining. n=6 to 8, each group. **F**, Brillouin frequency shift was obtained from myocardial sections of 24-week-old mice. n=4 to 11, each group. Data are shown as mean±SD. Multiple Mann-Whitney *U* tests followed by Bonferroni-Dunn posttest were used. Since there is no significant difference between WT and TMEM43wt mice, statistical comparisons between TMEM43wt and TMEM43mut or double transgenic mice are omitted to enhance the clarity of the plots. IVS indicates interventricular septum; LV, left ventricle; and RV, right ventricle.

strategy. To investigate whether late administration of the therapy could also ameliorate the ARVC5 phenotype, we administered AAV-WT-OPT to adult AAV-MUT mice after overt symptoms of the disease were already evident (10 weeks of age), including low LVEF, reduced QRS amplitude, and increased QRS duration. These mice were randomized into 2 groups with matched median LVEF and QRS amplitude. Mice from each group received the same dose of either AAV-LUC or AAV-WT-OPT used in neonates (1.7e13 VP/kg) via the femoral vein (Figure 8A). PCR analyses from 24-week-old mouse hearts exhibited sustained AAV-MUT and AAV-WT-OPT expression in both groups (Figure S6B).

Mice injected with AAV-WT-OPT showed a significant increase in LVEF compared with AAV-LUC-treated mice, lasting for up to 24 weeks (Figure 8B). Regarding QRS amplitude and duration, no significant improvement was observed (Figure 8C and 8D). During the 24-week follow-up period, none of the AAV-WT-OPT treated mice died, whereas 3 of 20 mice (15%) in the AAV-LUC group were found dead (Figure 8E), in line with our previous results at this age (Figure 6A). To uncover any subtle changes in electrical conduction, we administered a supratherapeutic dose of flecainide (40 mg/kg), a class I antiarrhythmic drug that can induce arrhythmias and produce AV block at high doses.[18] As shown in Figure 8F and 8G, AAV-WT-OPT treatment reduced the incidence of AV blocks in response to flecainide compared with treatment with AAV-LUC. These findings further support the potential of WT-TMEM43 overexpression therapy in improving cardiac function and electrical manifestations in ARVC5, even when administered in adult symptomatic mice.

DISCUSSION

Gene therapy approaches carrying functional copies of the affected genes, like the one used in this study, have shown to be a powerful tool for tailored therapy in a variety of genetic diseases. Some of these products have already been authorized for clinical practice,[19] including AAV-mediated expression of RPE65 for the treatment of retinal dystrophy, SMN1 for spinal muscular atrophy patients, or AADC for aromatic L-amino acid decarboxylase deficiency, among others.[20–22] Although no gene therapy has been approved for cardiac diseases yet, several gene therapy approaches are currently being developed for heart failure and genetic cardiomyopathies.[23] Specifically in ARVC, the potential of WT copy overexpression in PKP2-ARVC, the most common subtype of ARVC, has recently been demonstrated.[24,25] In fact, several products based on this new gene therapy strategy have received Food and Drug Administration approval for phase 1/2 clinical trials (https://www.clinicaltrials.gov; NCT05885412, NCT06109181, and NCT06228924).

Gene therapy approaches are usually designed as replacement therapies for biallelic or haploinsufficient diseases. When addressing dominant negative mutations like p.S358L in TMEM43, therapeutic strategies have mostly focused on antisense oligonucleotides and siRNAs that can downregulate the expression of both WT and affected gene copies, like inotersen, patisiran, and vutrisiran, authorized for targeting the TTR (transthyretin) mRNA in hereditary TTR-mediated amyloidosis.[26] However, silencing completely both the affected and unaffected gene copies might not be feasible in certain cardiac diseases, and alternative approaches are warranted. In this sense, our data suggest that functional copy overexpression should also be considered for the treatment of dominant negative diseases, such as ARVC5, without the need for knocking down the mutant allele.

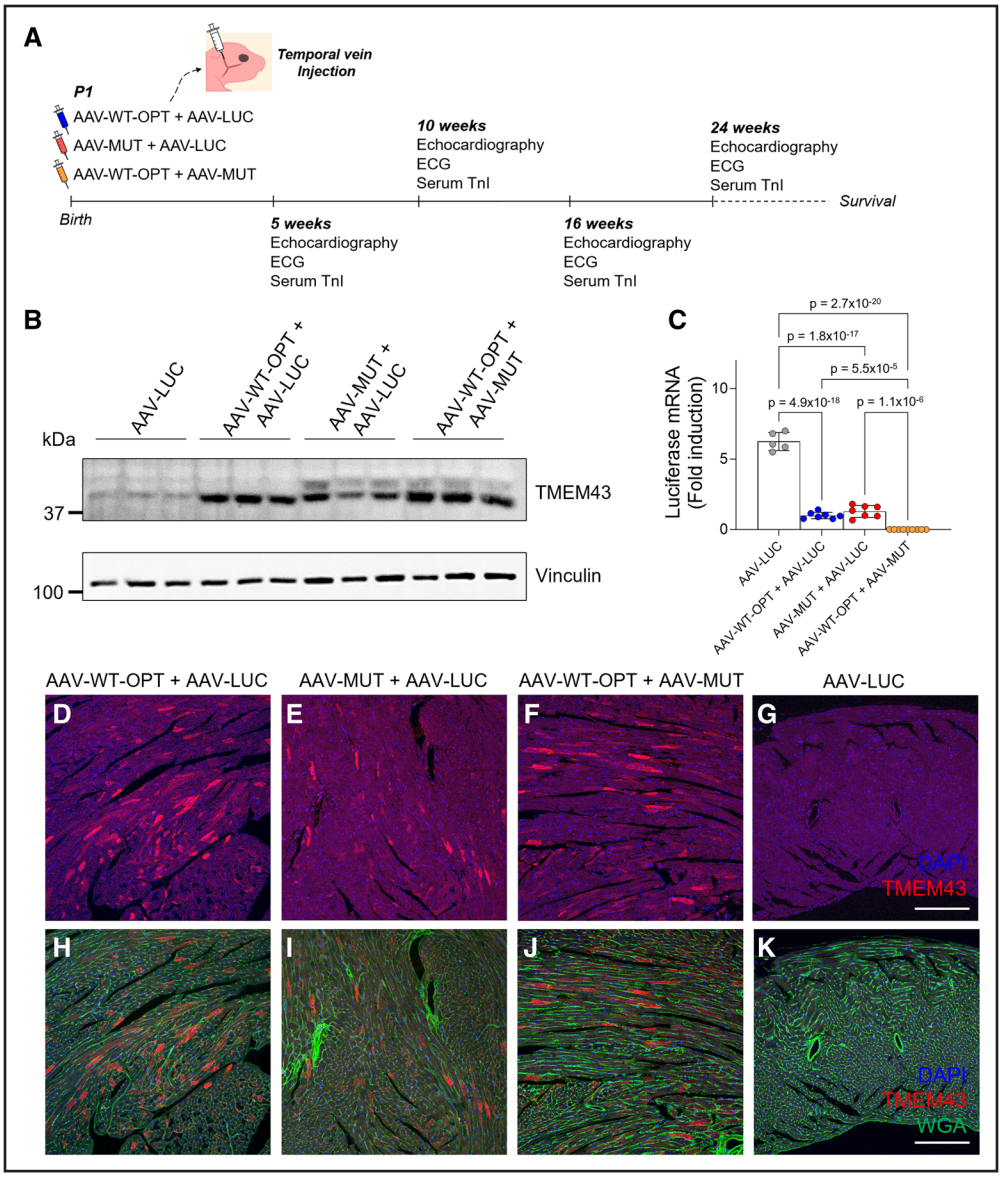

Figure 5. Delivery of codon-optimized wild-type (WT)-TMEM43 (transmembrane protein 43) using an adeno-associated viral vector (AAV) shows high expression in the myocardium.

A, Experimental design of self-complementary AAV administration and outcome analyses. A total viral load of 5e10 viral particles (VP) was administered into postnatal day 1 (P1) mice through the temporal vein as follows: AAV carrying TMEM43WT-OPT (AAV-WT-OPT)+AAV carrying luciferase (AAV-LUC; 2.5e10 VP each), AAV carrying S358L-TMEM43 (AAV-MUT)+AAV-LUC (2.5e10 VP each), or AAV-WT-OPT+AAV-MUT (2.5e10 VP each). **B**, TMEM43 expression was analyzed by western blot. n=6, each group. **C**, Luciferase mRNA expression levels were determined by quantitative reverse-transcribed polymerase chain reaction in 16-week-old mice hearts after intravenous delivery of AAV-LUC (5e10 VP/neonate), AAV-WT-OPT+AAV-LUC (2.5e10 VP/neonate each), AAV-MUT+AAV-LUC (2.5e10 VP/neonate each), or AAV-WT-OPT+AAV-LUC (2.5e10 VP/neonate each). n=5 to 9, each group. **D** through **G**, TMEM43 immunofluorescence analysis, and wheat germ agglutinin (WGA) co-stains in myocardial sections of 16-week-old mice after neonatal injection of AAVs; scale bar, 200 µm. Data are shown as mean±SD (**C**). One-way ANOVA was used, followed by Bonferroni posttest.

ARVC5 is an incurable disease, and current therapeutic options are limited to preventive or symptomatic treatments, aiming to avoid sudden cardiac death and heart failure.[3] In this regard, our group previously showed the potential of enalapril, a commonly used drug in heart failure patients, to preventively treat ARVC5.[27] However, although several models have been reported to date, no specific in vivo therapies targeting the primary cause of the disease have been proposed.[11,28–31]

The data presented here underscore the therapeutic potential of TMEM43 overexpression in ARVC5, with no apparent detrimental effects of TMEM43 overexpression in the heart under healthy conditions. In a first proof-of-concept approach, we generated a double transgenic mouse that overexpresses both WT and

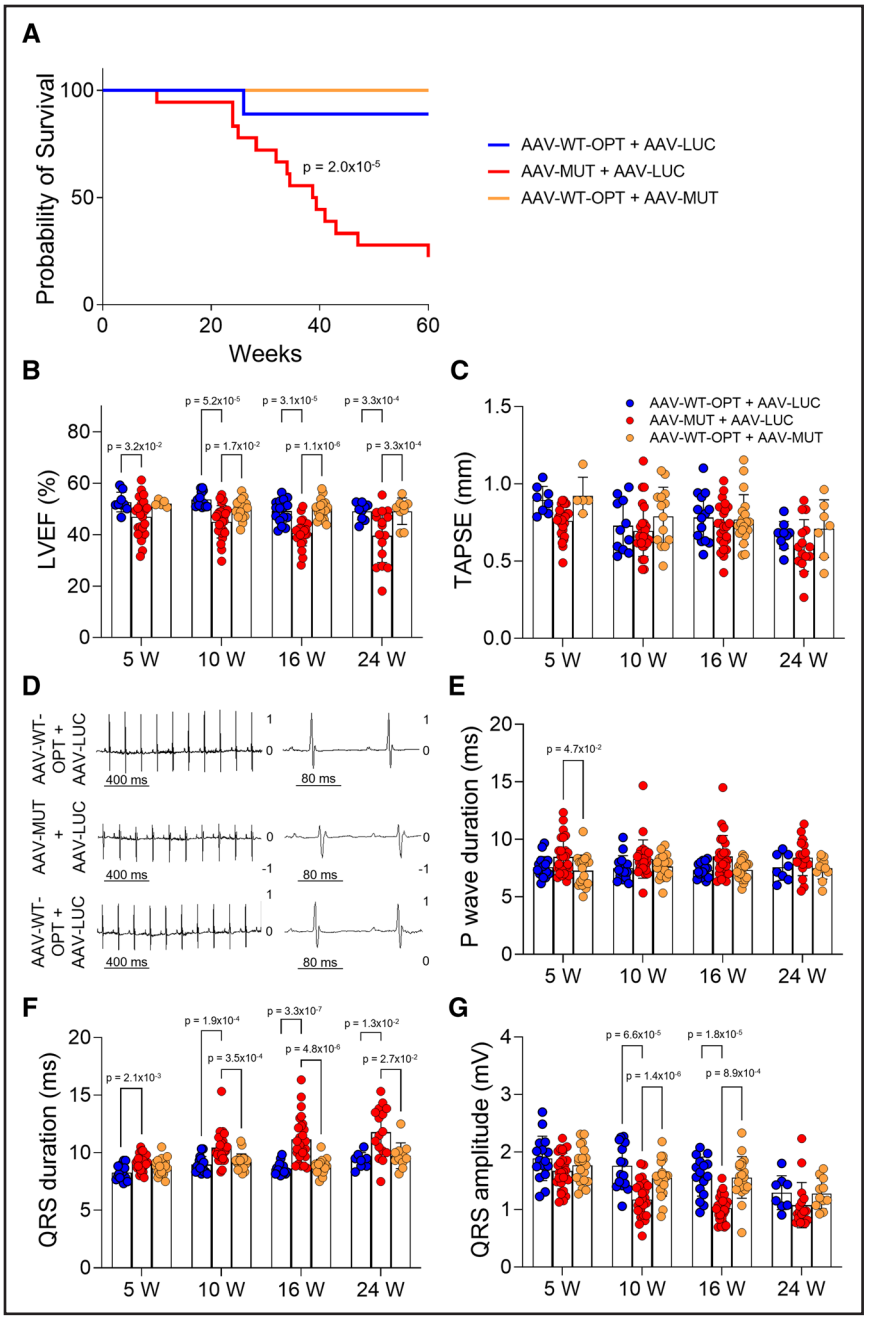

Figure 6. Early codon-optimized wild-type TMEM43 AAV vector (AAV-WT-OPT) administration improves life span, systolic function, and cardiac conduction defects.
A, Survival rate of AAV-WT-OPT+AAV vector expressing luciferase (AAV-LUC; n=12), AAV vector expressing S358L-TMEM43 (AAV-MUT)+AAV-LUC (n=19), and AAV-WT-OPT+AAV-MUT (n=13). The indicated *P* value was obtained with a log-rank test. **B** and **C**, Left ventricular ejection fraction (LVEF, **B**) and tricuspid annular plane systolic excursion (TAPSE, **C**) at 5, 10, and 16 weeks after AAV administration. **D** through **G**, Surface ECG at 16 weeks after AAV injection (**D**). P-wave duration (**E**) and QRS duration and amplitude (**F** and **G**) at 5, 10, 16, and 24 weeks after AAV injection. n=8 to 28, each group. Two-way ANOVA followed by Bonferroni posttest (**B** and **C**) or multiple Mann-Whitney *U* tests followed by Bonferroni-Dunn posttest (**E**, **F**, and **G**) were used.

mutant TMEM43 in cardiomyocytes. In a second, highly translational approach, we used AAVs to express WT and mutant human TMEM43 under the cardiac troponin T promoter. Both the transgenic mutant model and the mice infected with AAV-MUT recapitulated the main characteristics of the human disease, including cardiomyocyte death, ventricular dysfunction, and ECG abnormalities. Importantly, WT-TMEM43 overexpression successfully improved or delayed most of ARVC5 features in both settings, significantly increasing survival. This scenario resembles heterozygous mutations in channelopathies that lead to heteromeric assemblies carrying both WT and mutated subunits. In that context, the functional changes of the protein complex show a linear dependence on the number of mutant subunits in the complex.[32] Given these findings, we can speculate that TMEM43 works as a homomeric assembly and that overexpressing WT-TMEM43 in ARVC5 would increase the ratio of WT to mutant subunits, thereby reducing the functional impact of the mutant protein on the complex (see graphical abstract).

In addition to the p.S358L mutation, our optimized AAV-bearing WT-TMEM43 could potentially be applied to patients harboring different pathogenic or likely pathogenic variants in the *TMEM43* gene. Besides the S358L-TMEM43 variant causing ARVC5, 2 heterozygous missense variants, p.Glu85Lys and p.Ile91Val, affecting the hydrophilic domain of TMEM43, showed a

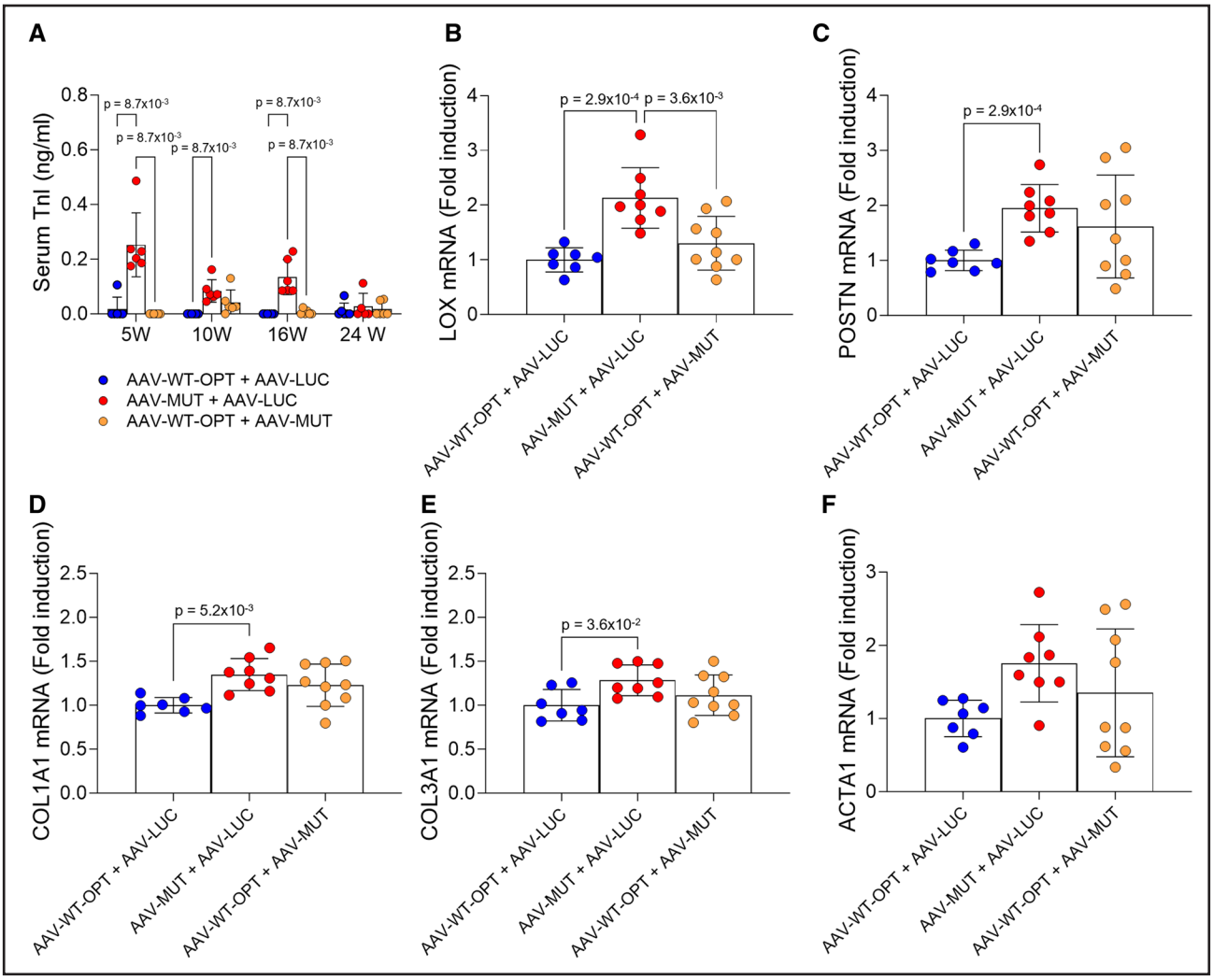

Figure 7. Codon-optimized wild-type TMEM43 AAV vector (AAV-WT-OPT) reduces cardiomyocyte necrosis and expression of fibrosis-related genes in mice.

A, Serum troponin I (TnI) by ELISA in mice at 5, 10, and 16 weeks of age. n=6, each group. **B** through **F**, mRNA expression levels of *LOX* (lysyl oxidase, **B**), *POSTN* (periostin, **C**), *COL1A1* (collagen type I alpha 1 chain, **D**), *COL3A1* (collagen type III alpha 1 chain, **E**) and *ACTA1* (alpha actin 1, **F**) quantified by quantitative reverse-transcribed polymerase chain reaction in 16 weeks old mouse hearts. n=7 to 9, each group. Data are shown as mean±SD. Multiple Mann-Whitney *U* tests followed by Bonferroni-Dunn posttest (**A**) or 1-way ANOVA (**B** through **F**) were used, followed by Bonferroni posttest. AAV-LUC indicates AAV vector expressing luciferase; and AAV-MUT, AAV vector expressing S358L-TMEM43.

phenotype of Emery-Dreifuss-related myopathy involving muscle atrophy with possible cardiac involvement.[33] In addition, a p.Arg372Ter nonsense mutation has been associated with deafness in an autosomal dominant auditory neuropathy spectrum disorder.[34] These variants showed decreased TMEM43 protein levels, suggesting that restoration of normal protein levels is likely to improve or prevent the pathological phenotype. Furthermore, gene therapy aimed at restoring TMEM43 expression could potentially be applied to other heart diseases that present TMEM43 downregulation, including cardiac hypertrophy or sepsis-induced cardiomyopathy.[35,36]

Here, we provide evidence that WT-TMEM43 overexpression improves cardiac function in ARVC5 by forming a WT-TMEM43-S358L-TMEM43 heterodimer and that a single systemic administration of our self-complementary myotropic AAV bearing codon-optimized WT-TMEM43 can prevent cardiomyocyte death and improve the disease in mice. While we acknowledge that more research is needed to comprehensively understand TMEM43 function and its role in heart disease, these results collectively suggest the therapeutic benefit of overexpressing WT-TMEM43 in cardiac and, potentially, noncardiac diseases beyond ARVC5.

Study Limitations

Although knock-in models are generally preferred for therapy development, heterozygous TMEM43-S358L knock-in models often show inconsistent results, with an exceedingly delayed onset or even an absence of cardiac phenotypes. Consequently, we used both transgenic and

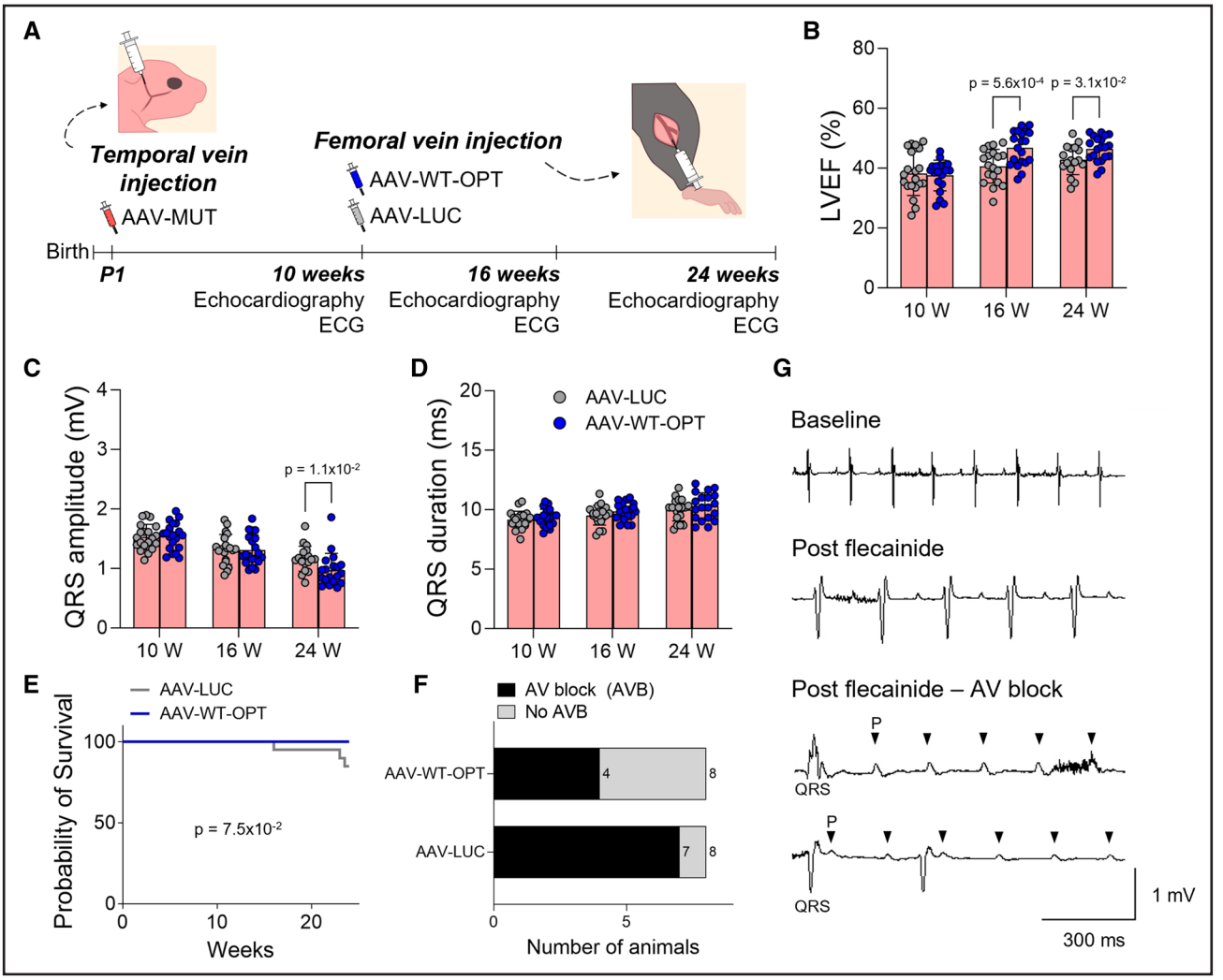

Figure 8. Codon-optimized wild-type TMEM43 AAV vector (AAV-WT-OPT) treatment in symptomatic arrhythmogenic right ventricular cardiomyopathy type 5 (ARVC5) adult mice improves systolic function and reduces arrhythmia susceptibility.
A, Experimental design of symptomatic ARVC5 mice treatment and outcome analyses. AAV vector expressing luciferase (AAV-LUC) or AAV-WT-OPT were administered into 10-week-old AAV vector expressing S358L-TMEM43 (AAV-MUT) mice through the femoral vein at 1.7e13 VP/kg. Left ventricular ejection fraction (LVEF, **B**), QRS duration (**C**), and QRS amplitude (**D**) before (10 W) and after (16 W, 24 W) AAV-WT-OPT or AAV-LUC administration in symptomatic AAV-MUT mice. n=17 to 20, each group. **E**, Survival rate of AAV-MUT mice treated with AAV-LUC or AAV-WT-OPT up to 24 weeks of age. n=20, each group. **F**, Number of mice showing AV block after flecainide administration. n=8, each group. **G**, ECG traces of 24-week-old mice at baseline, after flecainide, and after flecainide triggering AV block. Data are shown as mean±SD. Statistical significance of AAV-LUC vs AAV-WT-OPT was assessed with 2-way ANOVA followed by Bonferroni posttest (**B** and **D**), or with multiple Mann-Whitney *U* tests followed by Bonferroni-Dunn posttest (**C**).

AAV-based ARVC5 models, which reliably reproduce the key functional and electrophysiological abnormalities of the disease. Notably, the AAV-based model exhibited a milder phenotype, which we attribute to lower mutant protein expression compared with the transgenic model.

We propose that overexpression of WT TMEM43 confers a therapeutic benefit by increasing the ratio of WT to mutant subunits within TMEM43 oligomers; however, it remains unclear whether this benefit stems from the oligomerization process itself or from competitive interactions between WT and mutant subunits.

Furthermore, while our mouse gene therapy models have provided promising insights, significant challenges remain in translating these findings to larger mammals and ultimately to human patients. Differences in tissue structure, immune responses, and cardiac electrophysiology may impact the efficiency of AAV-based gene delivery, making future studies in larger animal models essential for clinical application.

ARTICLE INFORMATION

Received November 11, 2024; revision received February 18, 2025; accepted March 2, 2025.

Affiliations

Myocardial Homoestasis and Cardiac Injury Programme, Centro Nacional de Investigaciones Cardiovasculares Carlos III (CNIC), Madrid, Spain (L.L., M.A.-N.d.A.,

M.L.-O., J.I., P.M.-C., J.P.O., P.G.-P., E.L.-P.). Facultad de Veterinaria, Complutense University of Madrid, Spain (M.V.-O.). Instituto de Ciencia de Materiales de Madrid, Consejo Superior de Investigaciones Científicas, Spain (R.J.J.-R.). Unidad de Medicina y Cirugía Experimental, Instituto de Investigación Sanitaria Gregorio Marañón, Hospital Gregorio Marañón, Madrid, Spain (M.V.G.-G.). Department of Medicine and Life Sciences, Universitat Pompeu Fabra, Barcelona, Spain (P.M.-C.). Department of Pediatrics, University of Florida, Gainesville (B.J.B.). Heart Failure and Inherited Cardiac Diseases Unit, Department of Cardiology, Hospital Universitario Puerta de Hierro Majadahonda, Madrid, Spain (J.P.O., P.G.-P.). Centro de investigación Biomédica en Red Cardiovascular (CIBERCV), Madrid, Spain (P.G.-P., E.L.-P.).

Acknowledgments

We thank the Centro Nacional de Investigaciones Cardiovasculares animal facility for mouse breeding, the Viral Vectors Unit for AAV production and the Microscopy Unit for their support during image acquisition and analysis.

Sources of Funding

This study was funded by the Pathfinder Cardiogenomics program of the European Innovation Council of the European Union (DCM-NEXT project; project number: 101115416) and grants PID2021-124629OB-I00, TED2021-129774B-C22, and PLEC2022-009235 funded by the Ministry of Science and Innovation (MCIN/AEI/10.13039/501100011033), the European Union's NextGenerationEU/PRTR (Plan de Recuperación, Transformación y Resiliencia de España), and Fondo Europeo de Desarrollo Regional (FEDER) to E. Lara-Pezzi. The Centro Nacional de Investigaciones Cardiovasculares (CNIC) is supported by the Instituto de Salud Carlos III (ISCIII), the Ministerio de Ciencia, Innovación y Universidades (MICIU) and the Pro CNIC Foundation, and is a Severo Ochoa Center of Excellence (grant CEX2020-001041-S funded by MICIU/AEI/10.13039/501100011033).

Disclosures

The authors would like to acknowledge that this research has led to the filing of a pending patent application. Inventors: B.J. Byrne, M. Corti, E. Lara-Pezzi, L. Lalaguna, and P. García-Pavía. Application number: EP25382006.2. Title: Method for improving cardiac function in arrhythmogenic right ventricular cardiomyopathy type 5. Priority date: 08/01/2025. Applicants: Centro Nacional de Investigaciones Cardiovasculares Carlos III (F.S.P.), Fundación para la Investigación Biomédica del Hospital Universitario Puerta de Hierro Majadahonda, University of Florida Research Foundation, Incorporated.

Supplemental Material

Figures S1–S6
Major Resources Table
Unedited Immunoblots

REFERENCES

1. Corrado D, Basso C, Judge DP. Arrhythmogenic cardiomyopathy. *Circ Res*. 2017;121:785–802.
2. Arbelo E, Protonotarios A, Gimeno JR, Arbustini E, Barriales-Villa R, Basso C, Bezzina CR, Biagini E, Blom NA, de Boer RA, et al; ESC Scientific Document Group. 2023 ESC guidelines for the management of cardiomyopathies: developed by the task force on the management of cardiomyopathies of the European Society of Cardiology (ESC). *Eur Heart J*. 2023;44:3503–3626. doi: 10.1093/eurheartj/ehad194
3. Marcus FI, McKenna WJ, Sherrill D, Basso C, Bauce B, Bluemke DA, Calkins H, Corrado D, Cox MGPJ, Daubert JP, et al. Diagnosis of arrhythmogenic right ventricular cardiomyopathy/dysplasia: proposed modification of the task force criteria. *Eur Heart J*. 2010;31:806–814. doi: 10.1093/eurheartj/ehq025
4. James CA, Jongbloed JDH, Hershberger RE, Morales A, Judge DP, Syrris P, Pilichou K, Domingo AM, Murray B, Cadrin-Tourigny J, et al. International evidence based reappraisal of genes associated with arrhythmogenic right ventricular cardiomyopathy using the clinical genome resource framework. *Circ Genom Precis Med*. 2021;14:e003273. doi: 10.1161/CIRCGEN.120.003273
5. Merner ND, Hodgkinson KA, Haywood AFM, Connors S, French VM, Drenckhahn JD, Kupprion C, Ramadanova K, Thierfelder L, McKenna W, et al. Arrhythmogenic right ventricular cardiomyopathy type 5 is a fully penetrant, lethal arrhythmic disorder caused by a missense mutation in the TMEM43 gene. *Am J Hum Genet*. 2008;82:809–821. doi: 10.1016/j.ajhg.2008.01.010
6. Hodgkinson K, Connors SP, Merner N, Haywood A, Young TL, McKenna WJ, Gallagher B, Curtis F, Bassett AS, Parfrey PS. The natural history of a genetic subtype of arrhythmogenic right ventricular cardiomyopathy caused by a p.S358L mutation in TMEM43. *Clin Genet*. 2013;83:321–331. doi: 10.1111/j.1399-0004.2012.01919.x
7. Hodgkinson KA, Howes AJ, Boland P, Shen XS, Stuckless S, Young TL, Curtis F, Collier A, Parfrey PS, Connors SP. Long-term clinical outcome of arrhythmogenic right ventricular cardiomyopathy in individuals with a p.S358L mutation in TMEM43 following implantable cardioverter defibrillator therapy. *Circ Arrhythm Electrophysiol*. 2016;9:e003589. doi: 10.1161/CIRCEP.115.003589
8. Dominguez F, Zorio E, Jimenez-Jaimez J, Salguero-Bodes R, Zwart R, Gonzalez-Lopez E, Molina P, Bermúdez-Jiménez F, Delgado JF, Braza-Boïls A, et al. Clinical characteristics and determinants of the phenotype in TMEM43 arrhythmogenic right ventricular cardiomyopathy type 5. *Heart Rhythm*. 2020;17:945–954. doi: 10.1016/j.hrthm.2020.01.035
9. Haywood AFM, Merner ND, Hodgkinson KA, Houston J, Syrris P, Booth V, Connors S, Pantazis A, Quarta G, Elliott P, et al. Recurrent missense mutations in TMEM43 (ARVD5) due to founder effects cause arrhythmogenic cardiomyopathies in the UK and Canada. *Eur Heart J*. 2013;34:1002–1011.
10. Milting H, Klauke B, Christensen AH, Müsebeck J, Walhorn V, Grannemann S, Münnich T, Šarić T, Rasmussen TB, Jensen HK, et al. The TMEM43 Newfoundland mutation p.S358L causing ARVC-5 was imported from Europe and increases the stiffness of the cell nucleus. *Eur Heart J*. 2015;36:872–881. doi: 10.1093/eurheartj/ehu077
11. Padrón-Barthe L, Villalba-Orero M, Gómez-Salinero JM, Domínguez F, Román M, Larrasa-Alonso J, Ortiz-Sánchez P, Martínez F, López-Olañeta M, Bonzón-Kulichenko E, et al. Severe cardiac dysfunction and death caused by arrhythmogenic right ventricular cardiomyopathy type 5 are improved by inhibition of glycogen synthase kinase-3β. *Circulation*. 2019;140:1188–1204. doi: 10.1161/CIRCULATIONAHA.119.040366
12. Ruijter JM, Ramakers C, Hoogaars WMH, Karlen Y, Bakker O, van den Hoff MJB, Moorman AFM. Amplification efficiency: linking baseline and bias in the analysis of quantitative PCR data. *Nucleic Acids Res*. 2009;37:e45. doi: 10.1093/nar/gkp045
13. Sridharan D, Pracha N, Dougherty JA, Akhtar A, Alvi SB, Khan M. A one-stop protocol to assess myocardial fibrosis in frozen and paraffin sections. *Methods Protoc*. 2022;5:13. doi: 10.3390/mps5010013
14. Rioboó RJJ, Gontán N, Sanderson D, Desco M, Gómez-Gaviro MV. Brillouin spectroscopy: from biomedical research to new generation pathology diagnosis. *Int J Mol Sci* . 2021;22:8055. doi: 10.3390/ijms22158055
15. Villalba-Orero M, Jiménez-Riobóo RJ, Gontán N, Sanderson D, López-Olañeta M, García-Pavía P, Desco M, Lara-Pezzi E, Gómez-Gaviro MV. Assessment of myocardial viscoelasticity with Brillouin spectroscopy in myocardial infarction and aortic stenosis models. *Sci Rep*. 2021;11:24484. doi: 10.1038/s41598-021-04261-0
16. Weinmann J, Weis S, Sippel J, Tulalamba W, Remes A, El Andari J, Herrmann AK, Pham QH, Borowski C, Hille S, et al. Identification of a myotropic AAV by massively parallel in vivo evaluation of barcoded capsid variants. *Nat Commun*. 2020;11:1–12.
17. Inouye S, Sahara-Miura Y, Sato JI, Suzuki T. Codon optimization of genes for efficient protein expression in mammalian cells by selection of only preferred human codons. *Protein Expr Purif*. 2015;109:47–54.
18. Cerrone M, Noorman M, Lin X, Chkourko H, Liang FX, van der Nagel R, Hund T, Birchmeier W, Mohler P, van Veen TA, et al. Sodium current deficit and arrhythmogenesis in a murine model of plakophilin-2 haploinsufficiency. *Cardiovasc Res*. 2012;95:460–468. doi: 10.1093/cvr/cvs218
19. Shchaslyvyi AY, Antonenko SV, Tesliuk MG, Telegeev GD. Current state of human gene therapy: approved products and vectors. *Pharmaceuticals (Basel)*. 2023;16:1416. doi: 10.3390/ph16101416
20. Pearson TS, Gupta N, San Sebastian W, Imamura-Ching J, Viehoever A, Grijalvo-Perez A, Fay AJ, Seth N, Lundy SM, Seo Y, et al. Gene therapy for aromatic L-amino acid decarboxylase deficiency by MR-guided direct delivery of AAV2-AADC to midbrain dopaminergic neurons. *Nat Commun*. 2021;12:1–12.
21. Aslesh T, Yokota T. Restoring SMN expression: an overview of the therapeutic developments for the treatment of spinal muscular atrophy. *Cells*. 2022;11:417. doi: 10.3390/cells11030417
22. Maguire AM, Bennett J, Aleman EM, Leroy BP, Aleman TS. Clinical perspective: treating RPE65-associated retinal dystrophy. *Mol Ther*. 2021;29:442–463. doi: 10.1016/j.ymthe.2020.11.029
23. Argirò A, Ding J, Adler E. Gene therapy for heart failure and cardiomyopathies. *Rev Esp Cardiol (Engl Ed)*. 2023;76:1042–1054. doi: 10.1016/j.rec.2023.06.009

24. Bradford WH, Zhang J, Gutierrez-Lara EJ, Liang Y, Do A, Wang TM, Nguyen L, Mataraarachchi N, Wang J, Gu Y, et al. Plakophilin 2 gene therapy prevents and rescues arrhythmogenic right ventricular cardiomyopathy in a mouse model harboring patient genetics. *Nat Cardiovasc Res*. 2023;2:1246–1261. doi: 10.1038/s44161-023-00370-3
25. Kyriakopoulou E, Versteeg D, de Ruiter H, Perini I, Seibertz F, Döring Y, Zentilin L, Tsui H, van Kampen SJ, Tiburcy M, et al. Therapeutic efficacy of AAV-mediated restoration of PKP2 in arrhythmogenic cardiomyopathy. *Nat Cardiovasc Res*. 2023;2:1262–1276. doi: 10.1038/s44161-023-00378-9
26. Urits I, Swanson D, Swett MC, Patel A, Berardino K, Amgalan A, Berger AA, Kassem H, Kaye AD, Viswanath O. A review of patisiran (ONPATTRO®) for the treatment of polyneuropathy in people with hereditary transthyretin amyloidosis. *Neurol Ther*. 2020;9:301–315. doi: 10.1007/s40120-020-00208-1
27. Domínguez F, Lalaguna L, López-Olañeta M, Villalba-Orero M, Padrón-Barthe L, Román M, Bello-Arroyo E, Briceño A, Gonzalez-Lopez E, Segovia-Cubero J, et al. Early preventive treatment with enalapril improves cardiac function and delays mortality in mice with arrhythmogenic right ventricular cardiomyopathy type 5. *Circ Heart Fail*. 2021;14:e007616. doi: 10.1161/CIRCHEARTFAILURE.120.007616
28. Klinke N, Meyer H, Ratnavadivel S, Reinhardt M, Heinisch JJ, Malmendal A, Milting H, Paululat A. A Drosophila melanogaster model for TMEM43-related arrhythmogenic right ventricular cardiomyopathy type 5. *Cell Mol Life Sci*. 2022;79:444. doi: 10.1007/s00018-022-04458-0
29. Rouhi L, Cheedipudi SM, Chen SN, Fan S, Lombardi R, Chen X, Coarfa C, Robertson MJ, Gurha P, Marian AJ. Haploinsufficiency of Tmem43 in cardiac myocytes activates the DNA damage response pathway leading to a late-onset senescence-associated pro-fibrotic cardiomyopathy. *Cardiovasc Res*. 2021;117:2377–2394. doi: 10.1093/cvr/cvaa300
30. Gu Q, Xu F, Orgil BO, Khuchua Z, Munkhsaikhan U, Johnson JN, Alberson NR, Pierre JF, Black DD, Dong D, et al. Systems genetics analysis defines importance of TMEM43/ LUMA for cardiac- and metabolic-related pathways. *Physiol Genomics*. 2022;54:22–35. doi: 10.1152/physiolgenomics.00066.2021
31. Orgil BO, Munkhsaikhan U, Pierre JF, Li N, Xu F, Alberson NR, Johnson JN, Wetzel GT, Boukens BJD, Lu L, et al. The TMEM43 S358L mutation affects cardiac, small intestine, and metabolic homeostasis in a knock-in mouse model. *Am J Physiol Heart Circ Physiol*. 2023;324:H866–H880. doi: 10.1152/ajpheart.00712.2022
32. Brelidze TI. Heteromeric wild-type/mutant potassium channel subunit composition as a major determinant of channelopathy phenotype in heterozygous patients. *J Gen Physiol*. 2023;155:e202313333. doi: 10.1085/jgp.202313333
33. Liang WC, Mitsuhashi H, Keduka E, Nonaka I, Noguchi S, Nishino I, Hayashi YK. TMEM43 mutations in emery-dreifuss muscular dystrophy-related myopathy. *Ann Neurol*. 2011;69:1005–1013. doi: 10.1002/ana.22338
34. Jang MW, Oh DY, Yi E, Liu X, Ling J, Kim N, Sharma K, Kim TY, Lee S, Kim AR, et al. A nonsense TMEM43 variant leads to disruption of connexin-linked function and autosomal dominant auditory neuropathy spectrum disorder. *Proc Natl Acad Sci USA*. 2021;118:e2019681118. doi: 10.1073/pnas.2019681118
35. Chen Z, Cao Z, Gui F, Zhang M, Wu X, Peng H, Yu B, Li W, Ai F, Zhang J. TMEM43 protects against sepsis-induced cardiac injury via inhibiting ferroptosis in mice. *Cells*. 2022;11:2992. doi: 10.3390/cells11192992
36. Gu Y, Yao YR, Ding Y, Zhang XW. Reduced expression of transmembrane protein 43 during cardiac hypertrophy leads to worsening heart failure in mice. *Exp Biol Med (Maywood)*. 2023;248:1437–1445. doi: 10.1177/15353702231191111